Academia Open

Vol. 11 No. 1 (2026): June
DOI: 10.21070/acopen.11.2026.13959

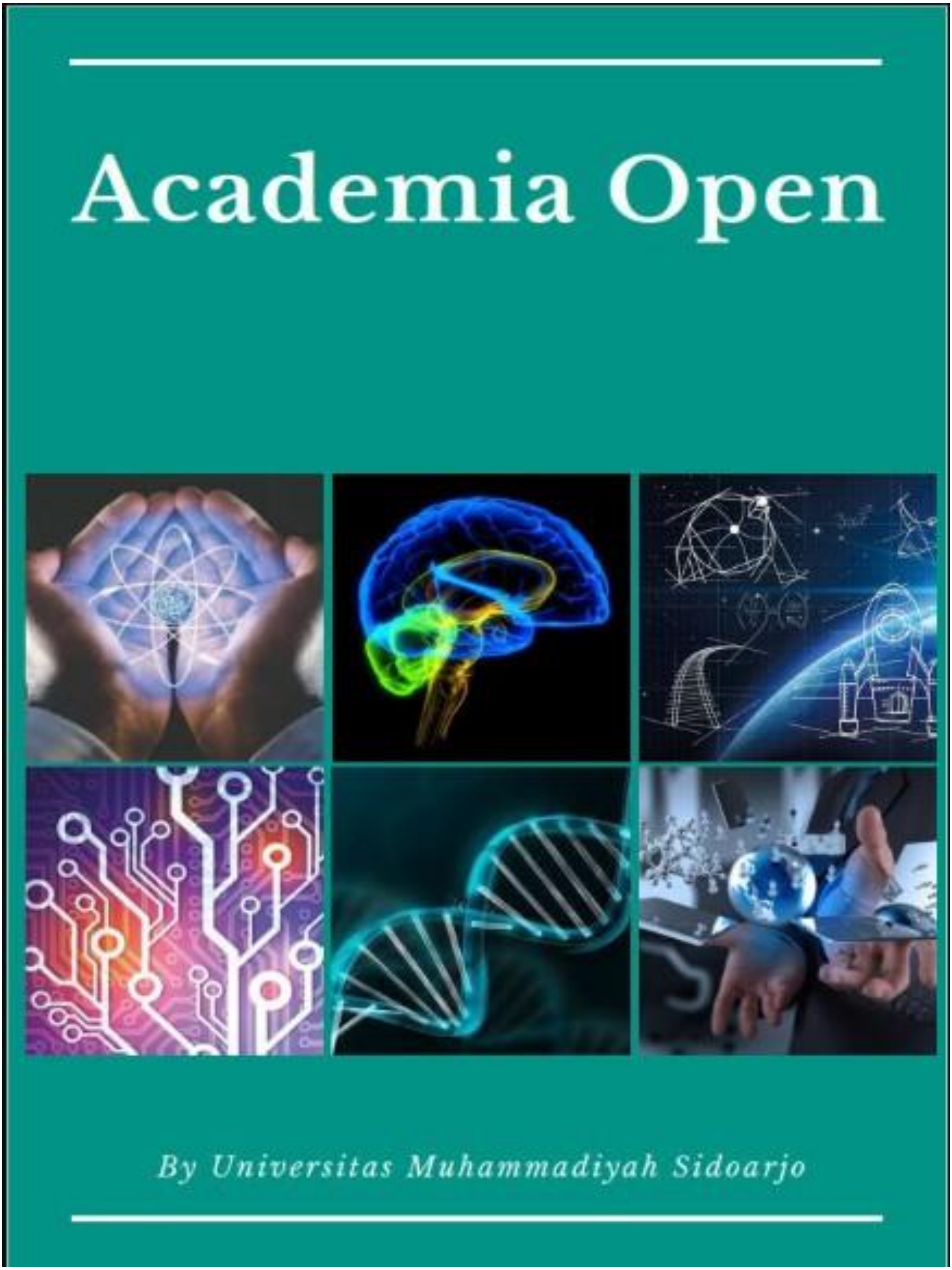

ISSN 2714-7444 (online), https://acopen.umsida.ac.id, published by Universitas Muhammadiyah Sidoarjo

Academia Open

Vol. 11 No. 1 (2026): June
DOI: 10.21070/acopen.11.2026.13959

Table Of Contents

ISSN 2714-7444 (online), https://acopen.umsida.ac.id, published by Universitas Muhammadiyah Sidoarjo

Originality Statement

Conflict of Interest Statement

Copyright Statement

Academia Open

Vol. 11 No. 1 (2026): June
DOI: 10.21070/acopen.11.2026.13959

EDITORIAL TEAM

Academia Open
Vol. 11 No. 1 (2026): June
DOI: 10.21070/acopen.11.2026.13959

Article information

Check this article update (crossmark)

Check this article impact [*]

Save this article to Mendeley

---

[*] Time for indexing process is various, depends on indexing database platform

Academia Open

Vol. 11 No. 1 (2026): June
DOI: 10.21070/acopen.11.2026.13959

Hybrid Composite of Inorganic Oxide (TiO2:WO3) for Remove Methyl Blue and Methyl Orange by Adsorption/Photo degradation Reaction

Baraa Kasim Mohammed, dr.baraa.kasim@kus.edu.iq (*)

Al-Karkh University of Science, College of Science, Forensic Department, Iraq

(*) Corresponding author

Abstract

General Background: Semiconductor inorganic oxides such as titanium dioxide and tungsten trioxide are widely used in environmental remediation due to their stability and photocatalytic properties for pollutant removal. **Specific Background:** Binary TiO_2:WO_3 composites provide synergistic semiconductor behavior supporting adsorption and ultraviolet-assisted photodegradation of dye pollutants in aqueous media. **Knowledge Gap:** However, comparative removal performance toward methyl orange and methylene blue using combined adsorption and photocatalytic processes remains insufficiently clarified. **Aims:** This study prepared a TiO_2:WO_3 composite using $TiOSO_4$ precipitation with hydrogen peroxide and evaluated its activity toward removal of methyl orange and methylene blue. **Results:** X-ray diffraction and Raman spectroscopy confirmed anatase, rutile, and WO_3 phases, while removal performance exceeded 80 percent for methyl orange and showed lower activity for methylene blue under combined processes. **Novelty:** The study demonstrates synergistic binary oxide activity supported by structural characterization and comparative dye removal behavior. **Implications:** The results support TiO_2:WO_3 composites as suitable materials for adsorption and photocatalytic dye removal applications in aqueous treatment systems.

Highlights:

- TiO_2 WO_3 Hybrid Structure Confirmed by XRD and Raman Characterization
- Binary Oxide System Shows Higher Removal Performance for Methyl Orange Than Methylene Blue
- Combined Adsorption and Ultraviolet-Assisted Reaction Achieves Removal Above 80 Percent

Keywords: Titanium Dioxide, Tungsten Trioxide, Binary Oxide Composite, Photodegradation, Dye Removal.

---

1. Introduction

Inorganic elements are chemically characterized by high stability and resilience, even under harsh conditions, which makes it suitable for many applications involving diverse and frequently changing chemical environments such Titanium Ti and Tungsten (W) [1-2]. However, a drawback is their ineffectiveness at normal temperatures, which limits their use in many applications, particularly in the energy and pollution removal sectors. The most commonly used method for activating these elements was to convert them into oxide form, where they are in a more chemically active form, such as TiO_2 and WO_3 [3]. According to details mentioned previously, many reactions or applications have become possible to accrue with high efficiency.

One method used to enhance the effectiveness of inorganic oxides, which still suffer from deficiencies in their activity, involves preparing inorganic complexes from their oxides. Some of these complexes are prepared by combining both oxides from their usual sources. [4]. Photocatalytic technologies are purifying on a huge scale for polluted water and air. The most common inorganic catalytic material for photoreaction is represented by titanium dioxide (TiO_2), which is effective for pollutant degradation due to two categories of (i) high photoexcitation activity: (i) chemical stabilization mechanisms and (ii) chemical stabilization mechanisms. The activities of TiO_2 were limited by the value of the band gap and the short time for forming (h+/e-) at the excitation state, which caused recombination for the two parts generated by the electron-hole in a very fast reaction. [5]. Many strategies were proposed and applied to solve or at least reduce the influence of the two limiting factors. Maybe creating a synergistic partnership with another semiconductor with a lower transfer rate or incentive, which is commonly referred to as a heterojunction [6]. Tungsten oxide (WO_3) is a semiconductor ideal for optoelectronics applications, with good conductivity, high value for e^-/h^+ mobility, and an oxygen-deficient n-type with an electronic bandgap of ~2.6–3.0 eV [7]. The hybrid-binary inorganic composite between short-wave UV light-absorbing TiO_2 and lower-energy-level near-visible-spectrum WO_3 creates new activity of the binary inorganic semiconductor. Photo-generated hole carriers left in the valence band under the presence of the corresponding TiO_2 levels will also have a strong reduction ability. The degree of holes and electrons. [8] In this work, a binary hybrid nanocomposite of inorganic oxides possessing semiconductor properties was prepared using WO_3 and precipitation TiO_2 after the addition of the substrate $TiOSO_4$ and precipitating agent. After preparing hybrid binary inorganic/semiconductor nanocomposites, the applications were done by removing two types of dyes, methyl orange and methylene blue, by adsorption and photodegradation reactions.

Experimental:

1- Chemicals

Titanyl sulfate ($TiOSO_4$), tungsten trioxide (WO_3), methyl orange (MO), and methylene blue (MB) were supplied by Sigma Chemical Company, with no further purifications. The precipitation reagent hydrogen peroxide (30% H_2O_2) was supplied from Barcelona, Scharlab, Spain. The scanning was analyzed with the UV-Vis spectrophotometer (TU-1950, Puxi General Instrument Co. Ltd., Beijing, China) from 200 to 800 nm. The value of pH of the prepared solutions was measured by LCD Display Tp-pH220 Potable pH Meter (Chongqing TOP Oil Purifier Co., Ltd., China) at 7.3 ±0.2 and was adjusted with (0.5 M) NaOH and (0.5 M) HCl. The concentration changes of the MO and MB solutions were represented by plotting the measured absorbance values into the standard curve equation.

2- Preparation of MO standard solution

1g of dye (MO) or (MB) were dissolved in less quantities of deionized water, stirred for 15 min at 350 rpm, and transferred with complete volume to a 1000 mL volumetric flask which represent (1000 ppm) of MO and MB standard solution respectively. MO and MB solutions was obtained by diluting the standard solution with deionized water. As shown in Fig.1 the Uv-visible spectrum for Prepared MO and MB solutions were measured its absorbance at wavelength 470 nm and 680 nm respectively by ultraviolet spectrophotometer.

Figure 1: Absorbance spectrum of (a) MO from wavelength (200-575 nm) and , (b) MB from (200-750 nm).

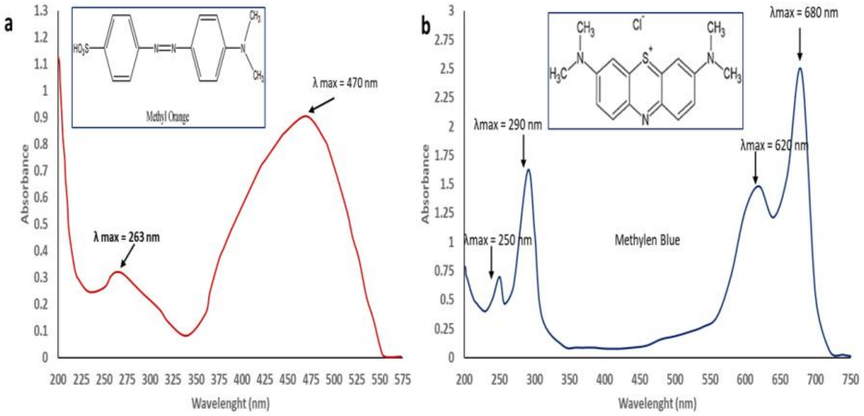

3- Synthesis of binary composites TiO2:WO3

The process includes preparing two solutions: the first, A, when (0.5) g of WO_3 was dispersed in 50 mL of distilled water with stirring by a magnetic stirrer (250 rpm) for 30 minutes. The second solution was B, which included the equivalent weight of $TiOSO_4$ to produce (1:1) {TiO_2:WO_3} dissolved in 50 mL of distilled water with heating to 40 degrees and continued stirring until forming a colorless solution. The two solutions, A and B, were mixed before 10 mL of 20% H_2O_2 was added slowly with stirring for 1 h. The mixture was still overnight before being filtered, and the precipitation materials were washed with distilled water. The yellow precipitation was dried at 100 degrees for 2 h before calcination at 400 degrees for 3 h.

4- Characterization

The x-ray diffraction XRD, measurements were carried out by (Philips APD 15) with CuKα radiation for 0.15405 nm, and the value of 2 thetas 10˚-80˚, with a scan rate of 5°/min and the resolution 0.02. Raman spectroscopy were measured by Sentara infinity 1 Broker at 530 nm, laser light, intensity 2m W for 5 lops per 2s and 3-5 cm of resolution. Fig. 2 shows XRD patterns of the WO_3 with the orthorhombic and monoclinic crystalline phases, which have distinguishable Bragg reflections (JCDPS. 20-1324) and (JCPDS. 01-072-1465). The diffraction peaks (2θ = 32°, 38°, 53°, and 64°) are assigned to the reflections associated with the tungsten oxide (WO_3) phase and Miller index (111), (211), (222), and (133) with crystallite sizes that were evaluated using the Scherrer formula [9]. XRD patterns for prepared TiO_2 were reported; high-intensity peaks demonstrate the sample mixture of anatase and rutile crystallinity, with a tetragonal structure. The Anatase phase included (2θ = 32, 35, 38, 47, 48, 57, 62, 64, 68, 69) with Miller index (101), (101), (200), (004), (211), (200), (211), (204), (216), and (220), while the Rutile phase was (2θ = 35, 56, and 57) and the Miller index was (101), (105), and (211) [10-11].

The XRD patterns for binary composites prepared by chemical deposition for TiO_2 from $Ti(SO_4)$ with WO_3 and then thermal treatment at 400°C include three new parts: the first was the anatase phase at (2θ = 25°, 38°, 47°, and 63°), which is related to (110), (101), (111), and (211). The second phase was rutile at (2θ = 53°, 55°, and 77°), which related to indices (101), (111), and (211). However, [12-13] the third was for WO_3 in binary, which witnessed reduced intensities of peaks as compared with TiO_2 and merged or overlapped peaks at 37°, 54°, and 64°. The diffraction peaks associated with WO_3, TiO_2, and TiO_2:WO_3 were calculated as crystallite sizes by the Scherrer formula and shown to be 12 nm, 19 nm, and 29 nm, respectively.

Figure 2: XRD- patterns of WO3, prepared TiO2, and prepared TiO2:WO3 for (2Θ=10˚-80˚).

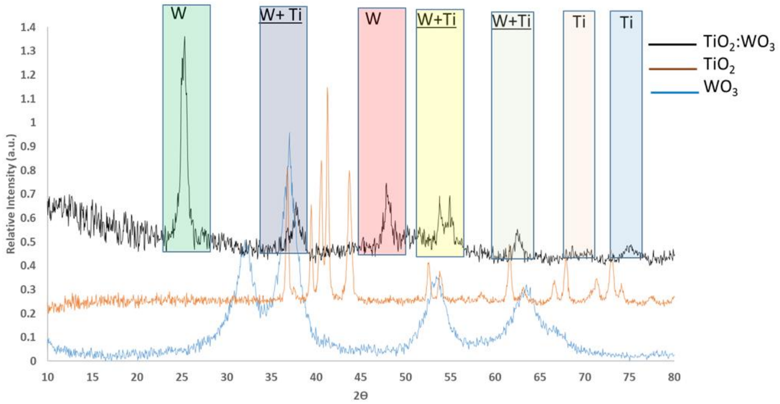

Raman spectra show strong peaks at 163–650 cm^{-1}, indicating the Ti–oxygen bonding, with vibration modes at 163 (Eg), 402 (B1g), 525 (A1g+B1g), and 650 (Eg, Bg, and Ag) due to symmetric stretching, symmetric, and antisymmetric bending vibration of TiO_2, respectively [14]. Pristine WO_3 showed the monoclinic phase, which has characteristic peaks at 426 and 860 cm^{-1}, and that represents the characterized peaks for the W=O bond. [15]. The Raman spectrum after doping WO_3 with TiO_2 showed the same detection for TiO_2 and WO_3 in the TiO_2/WO_3, with variance in the positions of peaks shifted for red shifted by approximately 3-7 cm^{-1}. In addition to 726 and 820 cm^{-1} for rutile TiO_2 and WO_3, respectively [16].

Figure 3: Raman spectrum of WO3, prepared TiO2, and prepared TiO2:WO3.

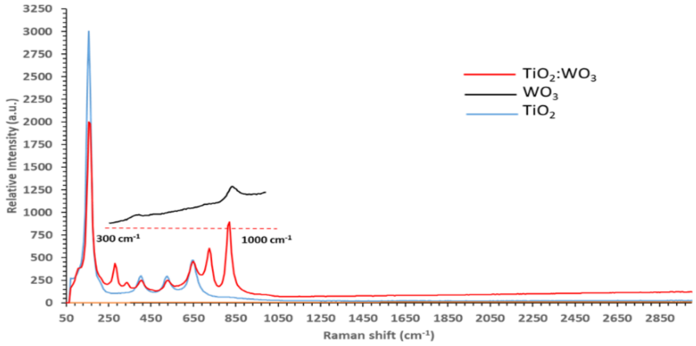

Adsorption and Photo-Degradation

The effectiveness of the binary composite was studied through a decolorization reaction, which requires two stages as shown in fig. 3: first, studying the adsorption activity, which precedes the second reaction; and second, studying the activity in the presence of ultraviolet radiation. The process was done with two dyes (20 ppm / 100 mL), MO and MB, and the same weight (60 mg) of catalysts WO_3, TiO_2, and TiO_2:WO_3. . Figure xx includes the scheme of the process, which contains a UV lamp (15 W) emitting radiation at 254 nm, which is enclosed in a wooden box.

Figure 4: skim for all experimental parts for dark and photo reaction.

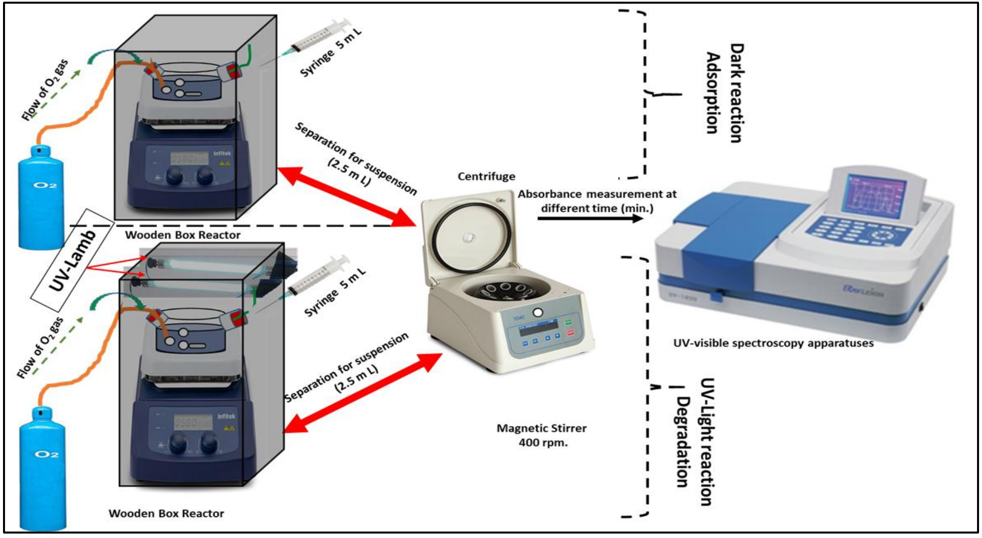

Figure 4 shows the two decolorization processes for MO, at adsorption, where the equilibrium time for decolorization was 45 min for the three due components TiO2, WO3, and TiO2:WO3 which showed decolorization rates ranging (WO3<TiO2<TiO2:WO3) respectively. The second process, photo reaction was witness the arrangement (TiO2<WO3<TiO2:WO3)

Figure 5: Adsorption and photo degradation of 20 ppm MO by 60 mg/ 100 m L TiO2 , WO3, and TiO2:WO3, at wavelength 470 nm and 298.15K.

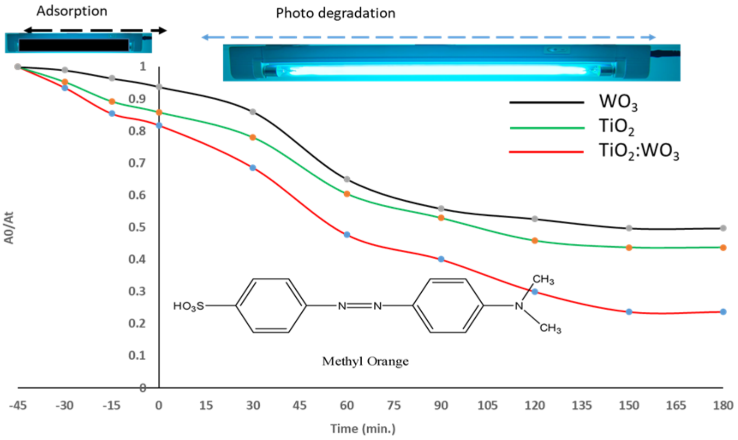

The behavior of three materials was shown change in activity with MB., according to the results in figure 5, the adsorption was (TiO2:WO3<WO3<TiO2), while photo reactions was (WO3<TiO2<TiO2:WO3).

Figure 6: Adsorption and photo degradation of 30 ppm MB by 60 mg/ 100 m L TiO2 , WO3, and TiO2:WO3, at wavelength 680 nm and 298.15K.

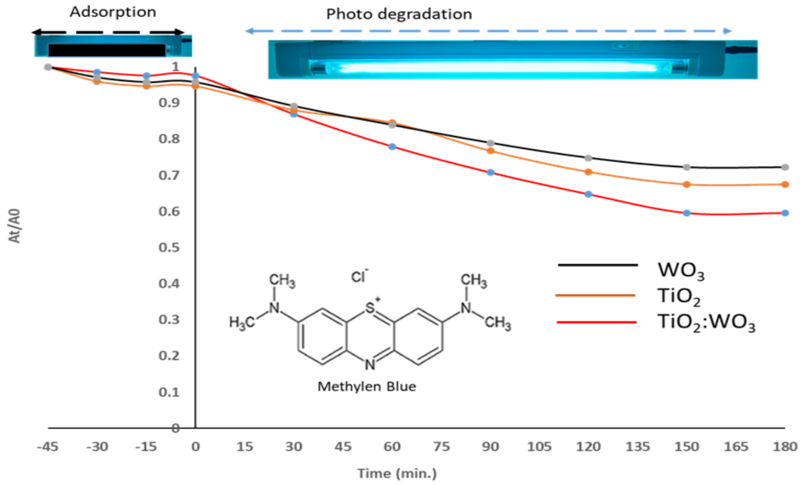

The activity of binary composite TiO2:WO3 towards removed MO and MB were reported in figure 6 with two process adsorption and photo reaction. The removal activity was more active with MO at the two process, in additions to variance in value for the two dyes.

Figure 7: The skim of (a) adsorption and photo degradation for 30 ppm MO and MB by 60 mg/100 m L of TiO2:WO3, with absorbance spectrum (a) MO, and (b) MB at wavelength 470 nm and 680 nm respectively.

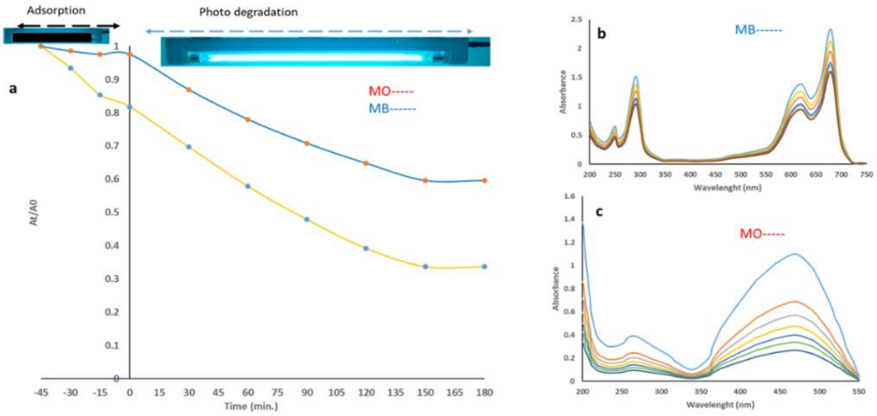

According to figure 7a, which mentions the values of percent removal %R [17] that is calculated by equation {%R=(At/A0)*100} in every process and total value. The results showed a greater adsorption advantage for the binary complex TiO_2:WO_3 in removing MO dyes compared to the individual components TiO_2 and WO_3. However, the photocatalytic reaction also showed an advantage for the binary complex, with the final removal yield reaching more than 80% of %R. The accumulation result in fig. 7b for MB showed less activity compared to the effect of pristine TiO_2, WO_3, and TiO_2:WO_3, which reached about 40% with MB, and that represents half the effectiveness of the same substance for removing MO.

Figure 8: The skim of %R (Adsorption+ Photo reaction) from 20 ppm of (a) MO, and (b) MB by (60 mg/ 100 m L) TiO2, WO3, and TiO2:WO3 at 298.15 K.

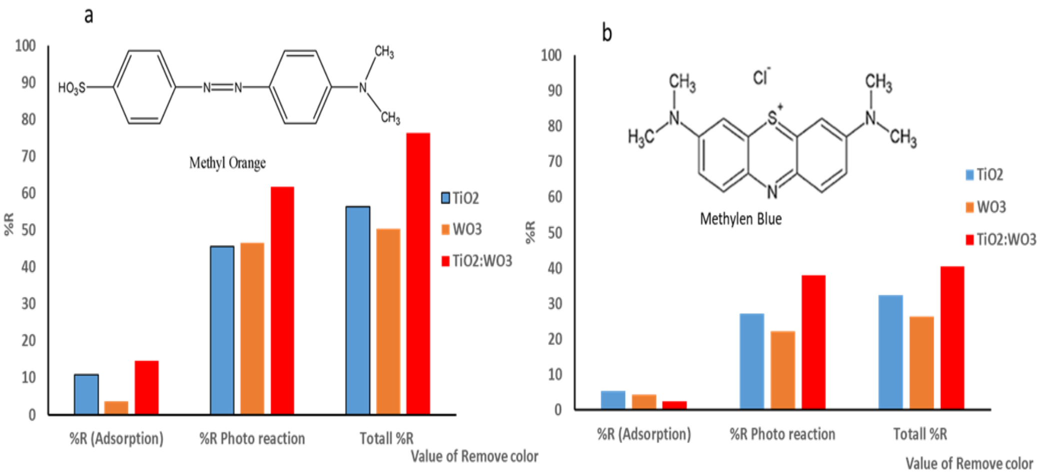

Mechanism of Reaction

Fig. 8 reported the proposal mechanism of photo-degradation by TiO_2:WO_3, which started with (-0.3 eV) for energy potential of the CB of anatase TiO_2 when proved for the synthesized process by XRD and Raman spectrum. The energy of UV irradiation was approximately 3.4 eV, which is a higher level than the band gap of WO_3 and TiO_2, with values of 2.7 eV and 3.2 eV, respectively. The level of UV energy is able to generate photons in both WO_3 and TiO_2, therefore it is a critical parameter to make the best separation between the excited electron and the positive hole with enough time to make the electron's delay from the hole for a suitable period of time to generate more active species [18].

The value as reported in the huge literature [19] is higher negative (0.74 eV) as compared with the CB energy for WO_3. The energy difference between the two inorganic oxides logically promotes the spontaneous transfer of electrons from TiO_2 towards WO_3 through CB [20]. Increasing the efficiency of the binary inorganic complex is another important factor that favors this behavior, represented by the continuous exchange of H+ between TiO_2 and WO_3 of each valence band in the two components. The factor that enhances electron transfer in the direction of the oxidation reaction is the presence of oxygen sites that are ready to receive electrons and prevent them from returning to the hole, which acts as an ideal capture for electrons [21]. The last inorganic behavior makes a real reaction to modifying and improving the efficiency for the surface of TiO_2 with WO_3.The presence of water molecules around the active oxidizing groups will have the effect of generating free hydroxyl radicals, which in turn act as active sites for the oxidation of dyes in general and MO in particular. The other inorganic parameter [22] reported in figure 7 was the higher value for VB of WO_3 as compared with the level of VB for TiO_2, and that makes h^+ of WO_3 a good recipient of H_2O molecules for easier oxidation and the formation of new free radicals (OH).

Figure 9: The skim for proposal mechanism for binary composite TiO2:WO3

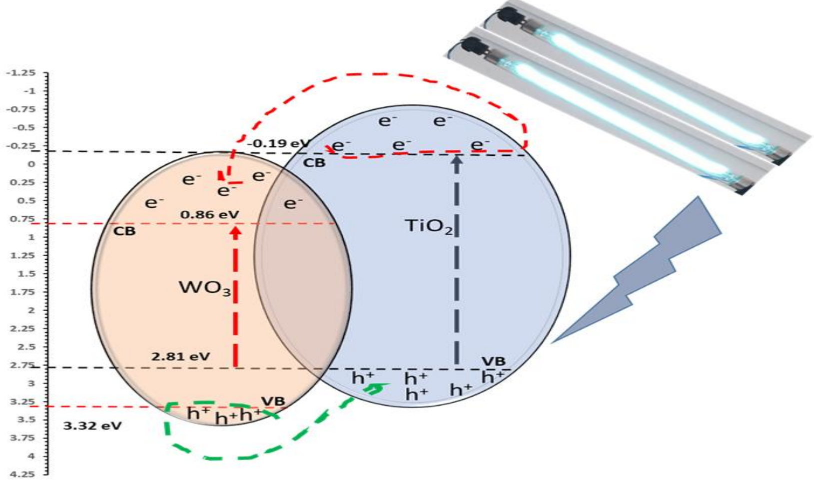

As demonstrated by the hybrid synergistic mechanism of the inorganic oxide, the two oxidants were unable to perform the same action to remove MB, which showed less activity compared to MO. The last behavior may be related to higher abilities for MO than MB, as shown in the adsorption results, which enhance the second part of removing dye [23]. The other cause was represented by high concentrations at 20 ppm and more, which converted the reaction likely in favor of removing MO more than MB due to the higher intensity of color, which prevented penetration of UV light [24]. Thus, according to the experimental section, the binary inorganic oxide hyper was more active with MO than MB.

Conclusion

The loading of titanium dioxide onto tungsten oxide was achieved by precipitating titanium ox-sulfate using hydrogen peroxide. This successfully established a bond and synergy between the two oxides, which was observed in both Raman spectroscopy and X-ray diffraction. The synergistic behavior was further demonstrated by the ability of the two non-organic complexes to decolorize the two dyes, despite the difference in efficiency between the two types. The synergistic effect between the inorganic oxides of tungsten and titanium was evident after a hybrid complex of the two was prepared. The effect was evident when the inorganic complex was more effective for adsorption and photodegradation compared to the two oxides when used individually. However, this did not prevent the MB dye from showing resistance to color removal compared to MO according to the conditions of the prepared hyper binary inorganic oxide composite.

References

1. B. Delaram , F. Mokari , M. Gholizadeh , ‘’ Use of the Advantages of Titanium in the Metal: Organic Framework. Titanium Alloys - Recent Progress in Design, Processing, Characterization, and Applications’’, 2023, IntechOpen. http://dx.doi.org/10.5772/intechopen.106947.
2. P. P, Ku.avat and P. Sonar and D. S. Dalal,''An overview on basics of organic and dye sensitized solar cells, their mechanism and recent improvements'', Renewable and Sustainable Energy Reviews, 2017, 78, pp.1262-1287, https://doi.org/10.1016/j.rser.2017.05.011.
3. S.D Mehta, N. Singh,'' Synthesis and applications of titanium oxide catalysts for lower temperature CO oxidation

'',Current Research in Green and Sustainable Chemistry, 2020, 3, 100022, DO - https://doi.org/10.1016/j.crgsc.2020.100022.

4. A. Chakib , A. Bekka , K. Mohamed , T. Wassila , I Kadi allah , J. A. Labrincha ,''Sol-Gel Synthesis of TiO2/WO3 and TiO2/WO3-graphene nanoparticles, investigation of their photocatalytic proprieties'', ChemRxiv. 2022; doi:10.26434/chemrxiv-2022-khqgj.
5. S.J. Armaković, M.M. Savanović, S. Armaković,'' Titanium Dioxide as the Most Used Photocatalyst for Water Purification'', An Overview. Catalysts 2023, 13, 26.https://doi.org/10.3390/catal13010026 .
6. A. Balapure, J. R. Dutta and R. Ganesan,'' Recent advances in semiconductor heterojunctions: a detailed review of the fundamentals of photocatalysis, charge transfer mechanism and materials'', RSC Appl. Interfaces, 2024, 1, 43.
7. Y. Yao ,D. Sang , L. Zou , Q. Wang, C. Liu,'' A Review on the Properties and Applications of WO3 Nanostructure-Based Optical and Electronic Devices,'' Nanomaterials (Basel). 2021 Aug 22;11(8):2136. doi: 10.3390/nano11082136. PMID: 34443966; PMCID: PMC8398115.
8. A. Rafiq, M. Ikram, S. Ali, F. Niaz, M. Khan, Q. Khan, M. Maqbool,''Photocatalytic degradation of dyes using semiconductor photocatalysts to clean industrial water pollution'', J. Indus. Eng. Chem., 97,2021, 111-128, https://doi.org/10.1016/j.jiec.2021.02.017.
9. Y. C. Liang, C.W. Chang,'' Preparation of Orthorhombic WO3 Thin Films and Their Crystal Quality-Dependent Dye Photodegradation Ability'', Coatings 2019, 9, 90. https://doi.org/10.3390/coatings9020090.
10. X. Han , B. Yao , K. Li, W. Zhu, and X. Zhang,'' Preparation and Photocatalytic Performances of WO3/TiO2 Composite Nanofibers'', J. Chem. 2020, Article ID 2390486, 12 pages https://doi.org/10.1155/2020/2390486.
11. A.K. John , S. P alaty, and S.S. Sharma,'' Greener approach towards the synthesis of titanium dioxide nanostructures with exposed {001} facets for enhanced visible light photodegradation of organic pollutants'', J Mater Sci: Mater Electron 31, 20868–20882 (2020). https://doi.org/10.1007/s10854-020-04602-1.
12. T. M. Jawad and L. M. Ahmed ,'' Synthesis of WO3/TiO2 nanocomposites for Use as Photocatalysts for Eosin Yellow Dye Degradation '', 2021 IOP Conf. Ser.: Mater. Sci. Eng. 1067 012153DOI 10.1088/1757-899X/1067/1/012153.
13. E. Perevedentseva,Y.C. Lin,A. Karmenyan, K.T. Wu, A. Lugovtsov, E. Shirshin, A. Priezzhev,C.L. Cheng,'' Raman Spectroscopic Study of TiO2 Nanoparticles' Effects on the Hemoglobin State in Individual Red Blood Cells'', Materials 2021, 14, 5920. https://doi.org/10.3390/ma14205920.
14. S.K. Yadav , P. Yadav, A.K. Vishwakarma,'' Study of microstructural, Raman spectra, and gas sensing properties of tungsten oxide'', J Porous Mater 32, 1321–1331 (2025). https://doi.org/10.1007/s10934-025-01771-4.
15. S.A. Evando , N.S. Victor,'' TiO2/WO3 heterogeneous structures prepared by electrospinning and sintering steps: Characterization and analysis of the impedance variation to humidity '', Journal of Advanced Ceramics 2019, 8(2): 238–246 https://doi.org/10.1007/s40145-018-0309-x.
16. A. J. Mohamed, A. Ibtesam, and H. A. Firas. "Compare studies for the photocatalytic degradation of thymol blue with synthesized and commercial MWCNTs." AIP Conference Proceedings. Vol. 2213. No. 1. AIP Publishing LLC, 2020.
17. L. Ernawati, R. A. Wahyuono, A. A. Muhammad, A. R. Nurislam Sutanto, I. K. Maharsih, N. Widiastuti, H. Widiyandari, Mesoporous WO3/TiO2 Nanocomposites Photocatalyst for Rapid Degradation of Methylene Blue in Aqueous Medium'', Inter. J. Engin A: Basics , 2019, 32(10),pp. 1345-1352.
18. M.A.S. Alothoum,''A Review of the Synthesis, Structural, and Optical Properties of TiO2 Nanoparticles: Current State of the Art and Potential Applications'', Crystals 2025, 15, 944. https://doi.org/10.3390/cryst15110944
19. C. Hou, and J. Hao,'' A three-dimensional nano-network WO3/F-TiO2- {001} heterojunction constructed with OH-TiOF2 as the precursor and its efficient degradation of methylene blue'', RSC Advances., 2021, 11, 26063–26072 .
20. M. Farzaneh, A., A. Mohammad,''Photocatalytic systems: reactions, mechanism, and applications'', RSC Advances,2024, 20609 - 20645,http://dx.doi.org/10.1039/D4RA03259D
21. L. Belhomme, M. Duttine, C. Labrugère, E. Coicaud, A. Rougier,'' Investigation of the photochromism of WO3, TiO2, and composite WO3-TiO2 nanoparticles. Inorganic Chemistry'', 2024, 63 (21), pp.10079-10091. ff10.1021/acs.inorgchem.4c01379ff. ffhal-04596811.
22. Y. He .,W. Bao , Y. Hua , Z. Guo , X. Fu , Bing Na , D. Yuan , C. Peng and H. Liu,'' Efficient adsorption of methyl orange and methyl blue dyes by a novel triptycene-based hyper-crosslinked porous polymer'', RSC Advances, 2022, 12, 9, pp. 5587-5594.
23. S. Kader, Md. Rashid Al-Mamun, Kabir Suhan, S. B. Shuchi, S. Islam,'' Enhanced photodegradation of methyl orange dye under UV irradiation using MoO3 and Ag doped TiO2 photocatalysts'', Environmental Technology & Innovation, 27, 2022, 102476, https://doi.org/10.1016/j.eti.2022.102476.
24. H. Liu , W. Guo , Y. Li , S. He and Chiyang He,''Photocatalytic degradation of sixteen organic dyes by TiO2/WO3-coated magnetic nanoparticles under simulated visible light and solar light' 'J. Envir. Chem. Engin.,6, 1, pp. 59-67, 2018. https://doi.org/10.1016/j.jece.2017.11.063.